Available online at www.eccomasproceedia.org
Eccomas Proceedia SMART (2023) 700-711

ECCOMAS
Proceedia

X ECCOMAS Thematic Conference on Smart Structures and Materials
SMART 2023
D.A. Saravanos, A. Benjeddou, N. Chrysochoidis and T. Theodosiou (Eds)

BENCHMARK OF OPTIMIZATION STRATEGIES FOR ACTUATOR PLACEMENT IN ADAPTIVE STRUCTURES

FRANCESCO VIRGILI, GENNARO SENATORE*, LUCIO BLANDINI

Institute for Lightweight Structures and Conceptual Design (ILEK)
University of Stuttgart
Pfaffenwaldring 14, 70569 Stuttgart, Germany
*Corresponding author: gennaro.senatore@ilek.uni-stuttgart.de

Abstract. Adaptive civil structures are mechanical systems that can modify the response caused by external actions. Civil structures must satisfy safety and serviceability criteria under strong and rare events and therefore are typically overdesigned for most of the service life. Previous work has shown that structural adaptation enables significantly better material utilization than conventional structures, reducing adverse environmental impacts of new construction. Adaptation can be performed through actuators integrated into the structural layout. Several methods have been formulated for actuator placement to maximize the efficacy of controlling displacements and the internal force flow. This paper offers a benchmark of two actuator placement strategies: 1) Gramian-based optimization of the actuator locations and commands to minimize the control error (i.e., maximize compensability) under general loading 2) constrained optimization to maximize response control efficacy under a set of external loads and subject to stress and actuation force limits. The benchmark metrics are energy requirements and control feasibility including the required number of actuators and force capacity. These two strategies often produce different actuator placements. The performance benchmark is carried out to provide a selection guideline in different scenarios.

Keywords: Adaptive structures, Active structural control, Actuator placement, Shape control, Force control, Steady-state disturbance compensability, Gramian optimization, high-rise.

1 INTRODUCTION

Buildings construction and operation are responsible for a substantial portion of global energy consumption, greenhouse gas emissions, and waste generation. The construction sector is a major consumer of mined raw materials leading to the depletion of resources once believed unlimited (e.g. sand, iron) [1]. The material used for construction causes 11% of the annual global CO2 emissions, and overall the building industry contributes to more than 36% of the global energy demand [2]. Addressing these challenges requires a change in the way buildings and civil structures, in general, are understood. Conventional civil structures must satisfy safety and serviceability criteria under strong and rare events and therefore are typically overdesigned for most of the service life. Instead, structures could be adaptive in response to changes in

© 2023 The Authors. Published by Eccomas Proceedia.
Peer-review under responsibility of the organizing committee of SMART 2023.
doi: 10.7712/150123.9824.450888

loading and other environmental actions [3]. The ability to reduce the response against strong but infrequent loading events enables material, embodied carbon and energy minimization, especially for stiffness-governed configurations such as tall and slender buildings and long-span bridges [4], [5]. Response mitigation under loading can also increase durability [6], which reduces maintenance and replacement needs.
Adaptation has been performed by linear actuators that are integrated into the structural layout. The action of linear actuators, e.g., length changes, has been employed to control the response of truss and frame configurations, including high-rise and bridge structures [5], [7]. Several actuator placement methods have been formulated to maximize the efficacy of controlling displacements and the internal force flow [8], [9]. This paper offers a benchmark of two actuator placement strategies to provide a selection guideline: 1) Gramian-based optimization of actuator placement and commands to minimize the control error (i.e., maximize compensability) under general loading [10]; 2) Constrained optimization of actuator placement and commands to maximize response control efficacy under a set of external loads and subject to stress and actuation force limits [9]. Section 2 gives the formulation for the structural and control models. Section 3 gives the formulation of two actuator placement methods. Section 4 benchmarks the actuator placement methods using a high-rise truss structure as a case study.

2 SYSTEM MODELLING

This work considers truss structures under the assumption of small deformations and linear elastic material. Under static loads, the system is described by:

$$\mathbf{K}\mathbf{q} = \mathbf{F} \tag{1}$$

where $\mathbf{K} \in \mathbb{R}^{n^{dof} \times n^{dof}}$ is the stiffness matrix, $\mathbf{q} \in \mathbb{R}^{n^{dof} \times 1}$ the nodal displacements and $\mathbf{F} \in \mathbb{R}^{n^{dof} \times 1}$ the external forces and n^{dof} the number of degrees of freedom. Actuation is achieved by fitting force serial liner actuators [11] in some of the truss elements to modify the internal forces and reduce displacements through controlled length changes. When the structural response is controlled, the external forces are distinguished into control $\mathbf{B}^u\mathbf{u}$ and disturbance forces $\mathbf{B}^z\mathbf{z}$:

$$\mathbf{F} = \mathbf{B}^u\mathbf{u} + \mathbf{B}^z\mathbf{z} \tag{2}$$

n^{act} denotes the number of actuators. The control input matrix $\mathbf{B}^u \in \mathbb{R}^{n^{dof} \times n^{act}}$ maps the control commands $\mathbf{u} \in \mathbb{R}^{n^{act} \times 1}$ (in this case length changes ΔL) onto equivalent loads, the disturbance matrix (or primary input matrix) $\mathbf{B}^z \in \mathbb{R}^{n^{dof} \times n^{dof}}$ describes the application of external disturbances $\mathbf{z} \in \mathbb{R}^{n^{dof} \times 1}$ (pressures, loads, temperature changes). The actuation force is in series with the force taken by the housing element, and thus the stiffness of the coupled system is:

$$\frac{1}{k} = \frac{1}{k^{el}} + \frac{1}{k^{act}} \tag{3}$$

Since the actuator stiffness k^{act} is typically much greater than the element stiffness k^{el}, the serial setup is dominated by the latter:

$$k = k^{el} = \frac{EA}{l_{eff}} \tag{4}$$

where A is the element cross-section area, E the Young modulus, and l_{eff} the effective length. For short truss elements and large cross-sections, the actuator stiffness might affect the serial stiffness and therefore should be considered.

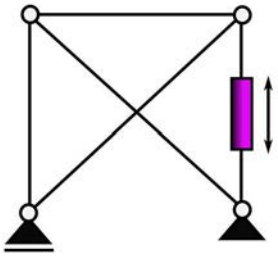

Figure 1 : Force Serial Actuation

Consider the truss structure illustrated in Figure 1, which is controlled with a linear actuator. The constitutive law of the assembly (element + actuator) is:

$$\Delta l = \Delta L + \frac{N}{k_i^{el}}, \tag{5}$$

where Δl is the total deformation which is sum of the actuator length change ΔL and the elastic extension (or contraction) caused by the element axial force N and k_i^{el} is the element stiffness. For clarity, the actuator length change ΔL is inelastic. The total extension of the element can be computed from the nodal displacements:

$$\Delta l = (\mathbf{B}_i^{eq})^T \mathbf{q}, \tag{6}$$

where $\mathbf{q} \in \mathbb{R}^{n^{dof} \times 1}$ is the vector of nodal displacements and $\mathbf{B}^{eq} \in \mathbb{R}^{n^{dof} \times n^{el}}$ is the equilibrium matrix containing the element direction cosines. Since the element force is opposite to that applied by the structure to the element, the virtual work of the conservative forces is [3]:

$$\begin{aligned} \delta W &= -N(\mathbf{B}_i^{eq})^T \delta q = \mathbf{P}_0 \delta q \\ \delta W &= (-\Delta l + \Delta L) k_i^{el} \left(\mathbf{B}_i^{eq}\right)^T \delta q \end{aligned} \tag{7}$$

Thus, the equivalent external load vector caused by an actuator length change ΔL is:

$$F^{act} = \mathbf{B}_i^{eq} k_i^{el} \Delta L \tag{8}$$

The control force consists of a pair of self-equilibrated forces applied by the active element to the connecting nodes, producing an inelastic displacement ΔL equivalent to a thermal deformation or a lack of fit [10]. Assuming n^{act} elements are active, the controlled system is described as:

$$\mathbf{Kq} = \mathbf{B}^z \mathbf{z} + \mathbf{B}^{eq} \mathbf{K}^{act} \mathbf{\Delta L} \tag{9}$$

where $\mathbf{K}^{act} \in \mathbb{R}^{n^{el} \times n^{act}}$ is an unconnected stiffness matrix (diagonal for a truss) containing the axial

stiffness of the active elements, and $\mathbf{\Delta L} \in \mathbb{R}^{n^{act} \times 1}$ is the actuator length change vector. The control input matrix can thus be written as:

$$\mathbf{B}^{u} = \mathbf{B}^{eq}\mathbf{K}^{act} \tag{10}$$

The internal element force changes $\mathbf{\Delta N} \in \mathbb{R}^{n^{el} \times 1}$ caused by actuation can be computed according to Eq.(5) and (6) as:

$$\mathbf{\Delta N} = (\mathbf{K}^{el}\mathbf{B}^{eq^{T}}\boldsymbol{q} - \mathbf{K}^{act})\mathbf{\Delta L} \tag{11}$$

where $\boldsymbol{K}^{el} \in \mathbb{R}^{n^{el} \times n^{el}}$ is an unconnected diagonal stiffness matrix containing the axial stiffness of all elements. Setting $\mathbf{z}$ to zero in Eq.(9), solving for $\mathbf{q}$ and substituting in Eq. (11), the internal force changes $\mathbf{\Delta N}$ caused by actuation can be expressed as:

$$\mathbf{\Delta N} = (\mathbf{K}^{el}\mathbf{B}^{eq^{T}}\mathbf{K}^{-1}\mathbf{B}^{u} - \mathbf{K}^{act})\mathbf{\Delta L} \tag{12}$$

For notation consistency the actuator length changes $\mathbf{\Delta L}$ will be denoted as $\mathbf{u}$, and control input and actuator length changes will be used interchangeably.

3 ACTUATOR LAYOUT OPTIMIZATION

The determination of an efficient actuator placement is typically a combinatorial optimization problem that involves selecting a subset from a finite set of possible placements. When all elements are candidate sites for actuators, the number of placements increases exponentially with the number of structural elements:

$$\sum_{n^{act}=1}^{n^{el}} \left(\frac{n^{el}}{n^{act}!\left(n^{el} - n^{act}\right)!} \right) \simeq 2^{n^{el}} \tag{13}$$

Computation of all possible sets is not feasible, the solution space of the optimization problem must be explored through optimization methods that involve heuristics, mixed-integer formulations [12] or integer relaxation approaches[13].

3.1 Actuator placement based on compensability Gramian

An optimization formulation for actuator placement based on the disturbance compensability Gramian is given in [10]. The formulation is given as independent of a specific disturbance (i.e., set of load cases) and for a total reduction of displacements (zero output vector). The method is here reformulated for multiple load cases and to account for constraints on forces and displacements. The control system is given by:

$$\begin{cases} \boldsymbol{K}\mathbf{q}_{j} = \mathbf{B}^{u}\mathbf{u}_{j} + \mathbf{B}^{z}\mathbf{z}_{j} \\ \mathbf{y}_{j} = \mathbf{C}\ \mathbf{q}_{j} + \mathbf{D}\ \mathbf{u}_{j} \end{cases} \tag{14}$$

where $\mathbf{y}_{j} \in \mathbb{R}^{n^{y}}$ is the system output vector for load case j, $\mathbf{C} \in \mathbb{R}^{n^{y} \times n^{dof}}$ the output matrix describing the relationship between the system state variables $\mathbf{q}_{j}$ and output variables $\mathbf{y}_{j}$, $\mathbf{D} \in \mathbb{R}^{n^{y} \times n^{act}}$ the feedthrough matrix describing the coupling between the control inputs $\mathbf{u}_{j}$ and

outputs $\mathbf{y}_j$. The output error $\mathbf{e}_j \in \mathbb{R}^{n^y \times 1}$ is given with respect to the serviceability limit states $\mathbf{y}_j^{SLS}$, which is the target output:

$$\begin{aligned} &\mathbf{e}_j = (\mathbf{y}_j^{SLS} - \mathbf{y}_j) = \\ &\mathbf{e}_j = \mathbf{C}_j^{SLS}\mathbf{K}^{-1}\mathbf{B}^z\mathbf{z}_j - \left(\mathbf{C}\mathbf{K}^{-1}\mathbf{B}^u + \mathbf{D}\right)\mathbf{u}_j \\ &\forall\ \mathbf{y}_j^{SLS} \neq \mathbf{0} \end{aligned} \tag{15}$$

where $\mathbf{C}_j^{SLS} \in \mathbb{R}^{n^y \times n^{dof}}$ is the target output matrix, which is determined for each load case.
The optimal control input to obtain the target output is given by:

$$\mathbf{u}_j = \left(\mathbf{C}\mathbf{K}^{-1}\mathbf{B}^u + \mathbf{D}\right)^+ \left(\mathbf{C}_j^{SLS}\mathbf{K}^{-1}\mathbf{B}^z\right)\mathbf{z}_j \tag{16}$$

where $(\cdot)^+$ denotes the pseudoinverse operator. The minimum output error can be written as:

$$\begin{aligned} &\mathbf{e}_j^* = \mathbf{H}_j\mathbf{z}_j \\ &\mathbf{H}_j = \left(\left(\mathbf{C}\mathbf{K}^{-1}\mathbf{B}^u + \mathbf{D}\right)^+ \cdot \left(\mathbf{C}\mathbf{K}^{-1}\mathbf{B}^u + \mathbf{D}\right) - \mathbf{I}\right) \cdot \left(\mathbf{C}_j^{SLS}\mathbf{K}^{-1}\mathbf{B}^z\right) \end{aligned} \tag{17}$$

where $\mathbf{H}_j \in \mathbb{R}^{n^y \times n^{dof}}$. The minimum squared error is obtained through a L^2 -norm:

$$\left\|\mathbf{e}_j^*\right\|_2^2 = \mathbf{e}_j^{*T}\mathbf{e}_j^* = (\mathbf{z}_j^T\mathbf{H}^T\mathbf{H}\mathbf{z}_j) = \mathbf{z}_j^T\mathbf{W}\,\mathbf{z}_j \tag{18}$$

$\mathbf{W} \in \mathbb{R}^{n^y \times n^y}$ is denoted as the disturbance-independent compensability Gramian. When accounting for specific disturbances, the compensability Gramian $\tilde{\mathbf{W}}_j \in \mathbb{R}^{n^y \times n^y}$ for the load case $\mathbf{z}_j$ is obtained as a symmetric matrix of inner products $\left\langle e_{ji}^* e_{jk}^{*T} \right\rangle\ \forall i,k$:

$$\mathbf{e}_j^*\mathbf{e}_j^{*T} = \widetilde{\mathbf{W}}_j \tag{19}$$

Given a set of actuator locations $S^{act} \in \{0,1\}^{n^{el}}$, $\widetilde{\mathbf{W}}_j$ quantifies the efficacy of the actuator placement S^{act} to achieve minimum output error. When the i^{th} entry of S^{act} is 1, it indicates that the i^{th} element houses an actuator and 0 otherwise. Different metrics can be formulated to evaluate the efficacy of a set of actuators to compensate for the effect of disturbances. For example, the Gramian $\tilde{\mathbf{W}}_j$ minimum and maximum eigenvalues ($\lambda_{\min}(\widetilde{\mathbf{W}}_j), \lambda_{\max}(\widetilde{\mathbf{W}}_j)$), the determinant $\det(\widetilde{\mathbf{W}}_j)$ and the trace $\mathrm{tr}(\widetilde{\mathbf{W}}_j)$. It can be shown that [14]:

$$\lambda_{\min}(\widetilde{\mathbf{W}}_j) \leq \frac{n}{\mathrm{tr}(\widetilde{\mathbf{W}}_j^{-1})} \leq (\det(\widetilde{\mathbf{W}}_j))^{\frac{1}{n}} \leq \frac{1}{n}\mathrm{tr}(\widetilde{\mathbf{W}}_j) \leq \lambda_{\max}(\widetilde{\mathbf{W}}_j),\ \forall j \tag{20}$$

While the trace and the determinant are proportional to the average squared input error norm, the minimum and maximum eigenvalues quantify the upper and lower bounds on the squared error norm. A cost function is defined for each actuator set S^{act} and each load case j.

$$\mathrm{tr}\left(\widetilde{\mathbf{W}}_j\right)_{S^{act}} = \left\|\mathbf{e}_j^*\right\|_2^2 = J\left(S^{act}\right)_j \tag{21}$$

$J\left(S^{act}\right)_j$ is then normalized with respect to the uncontrolled state $J(0)_j$:

$$J^{\|}\left(S^{act}\right)_j = \frac{J(0)_j - J(S)_j}{J(0)_j} \tag{22}$$

$J^{\|}\left(S^{act}\right)_j$ takes value in the range [0,1], and $J^{\|}\left(S^{act}\right)_j = 1$ when the control error is zero. $J^{\|}\left(S^{act}\right)_j$ is further averaged over the number of load case n^{LC} :

$$J^{\|}\left(S^{act}\right) = \frac{\sum_{j}^{n^{LC}} J^{\|}(S)_j}{n^{LC}} \tag{23}$$

The actuator layout optimization problem is formulated as:

$$\min_{S^{act}} \left(1 - J^{\|}\right) \quad s.t. \quad \begin{cases} \|\boldsymbol{y}_j\| \le \|\boldsymbol{y}^{SLS}\| \\ \underline{F}^{act} < F^{act}_{\max,j} < \bar{F}^{act} \\ E^{act}_j < \bar{E}^{act} \end{cases} \quad \forall\, j \in \left[1, n^{LC}\right] \tag{24}$$

where $\underline{F}^{act}$ and $\bar{F}^{act}$ are upper and lower bounds for the maximum actuator force $F^{act}_{\max,j}$, $\bar{E}^{act}$ the upper bound for the control energy E^{act}_j. A Greedy algorithm is implemented to solve the problem stated in (24). Starting from a set that includes all elements (i.e., all elements are active), $J^{\|}(S^{act})_j$ is computed by removing each actuator in turn $s = \{1 \ldots n^{el} - 1\}$. The actuator removal that causes the least deterioration of $J^{\|}(S^{act})_j$ is evaluated, and the corresponding actuator index is removed from the set. Similarly, the Greedy algorithm can be implemented in the reverse direction, i.e., starting from an empty set and adding the actuator that gives the greatest improvement to the objective function. The solution that satisfies the target output using the minimum number of actuators is selected. For brevity, the disturbance-independent compensability Gramian optimization method given in [10] is denoted with D.I.C.G.O. while with C.G.O. the load-dependent reformulation that is given in this work.

Unconstrained displacement control

$$\mathbf{u}_j = \left(\mathbf{C}_{cdof}\mathbf{K}^{-1}\mathbf{B}^u\right)^{+}\left(\mathbf{C}^{SLS}_{cdof,j}\mathbf{K}^{-1}\mathbf{B}^z\right)\mathbf{z}_j \tag{25}$$

where $\mathbf{C}_{cdof} \in \mathbb{R}^{n^{cdof} \times n^{dof}}$ is the output matrix reduced to the controlled degrees of freedom and the target output matrix $\mathbf{C}^{SLS}_{cdof,j} \in \mathbb{R}^{n^{cdof} \times n^{dof}}$ scales the uncontrolled displacements to the target displacements. The output error can thus be written as:

$$\mathbf{e}^{*}_j = \left(\left(\mathbf{C}_{cdof}\mathbf{K}^{-1}\mathbf{B}^u\right)^{+} \cdot \left(\mathbf{C}_{cdof}\mathbf{K}^{-1}\mathbf{B}^u\right) - \mathbf{I}\right) \cdot \left(\mathbf{C}^{SLS}_{cdof,j}\mathbf{K}^{-1}\mathbf{B}^z\right)\mathbf{z}_j \tag{26}$$

Unconstrained force control

For sufficiently redundant structures it is possible to achieve an optimal internal force distribution through actuation. Since controlling a limited set of internal forces could cause the

overloading of some of the uncontrolled elements, it is preferable to consider all internal forces:

$$\mathbf{C}^N = (\mathbf{K}^{el}\mathbf{B}^{eqT}) \tag{27}$$

$\mathbf{C}^N \in \mathbb{R}^{n^{el} \times n^{dof}}$ returns the element internal forces. Previous work [13] has shown that an efficient strategy is to set as target load-path one that satisfies force equilibrium without accounting for geometric compatibility:

$$\mathbf{N}^* = (\mathbf{B}^{eq})^+ \mathbf{z}_j \tag{28}$$

This is possible because geometric compatibility will be satisfied through the deformation caused by the actuator length changes. Note that $\mathbf{N}^*$ might not satisfy stress limits, which can be met by adding further constraints (see Eq.(38)). The feedthrough matrix accounts for the contribution of the inelastic length change of the actuators to the total element length change:

$$\mathbf{D} = -\mathbf{K}^{act} \tag{29}$$

The optimal actuator commands are obtained as:

$$\mathbf{u}_j = \left(\mathbf{C}^N \mathbf{K}^{-1} \mathbf{B}^u + \mathbf{D}\right)^+ (\mathbf{B}^{eq})^+ \mathbf{z}_j \tag{30}$$

The output error is given by:

$$\mathbf{e}_j^* = \left(\left(\mathbf{C}^N \mathbf{K}^{-1} \mathbf{B}^u + \mathbf{D}\right)^+ \cdot \left(\mathbf{C}^N \mathbf{K}^{-1} \mathbf{B}^u + \mathbf{D}\right) - \mathbf{I}\right) \cdot (\mathbf{B}^{eq})^+ \mathbf{z}_j \tag{31}$$

3.2 Actuator placement based on constrained input optimization

An actuator placement method based on constrained input optimization is given [13]. In [13] the problem is presented as a constrained minimization in which the number of actuators n^{acts} is set to the number of controlled degrees of freedom n^{cdof} plus the static indeterminacy r:

$$n^{act} = n^{cdof} + r \tag{32}$$

which is the number of releases required to transform a statically indeterminate structure into a controlled mechanism [13]. However, a lower number of actuators is often required to satisfy displacement and stress limits, as also shown in [15]. The optimization variable is the actuator command $\mathbf{u} \in \mathbb{R}^{n^{act}}$ that modifies the response from the uncontrolled state $\left\{\mathbf{y}_j^0, \mathbf{N}_j^0\right\}$ with the target displacement correction $\Delta\mathbf{y}_j^{SLS}$ and ensuring a geometrically compatible load path redirection $\Delta\mathbf{N}_j^*$:

$$\begin{aligned} &\min_{\mathbf{u}} \left\| \mathbf{S}^q \mathbf{u}_j - \Delta\mathbf{y}_j^{SLS} \right\|_2 \\ &s.t. \quad \mathbf{S}^N \mathbf{u}_j = \Delta\mathbf{N}_j^* \\ &\qquad \underline{\mathbf{u}} \le \mathbf{u} \le \bar{\mathbf{u}} \end{aligned} \tag{33}$$

where $\mathbf{S}^q \in \mathbb{R}^{n^{cdof} \times n^{act}}$ and $\mathbf{S}^N \in \mathbb{R}^{n^{el} \times n^{act}}$ are the displacement and force sensitivity (or influence) matrices, and $\{\underline{\mathbf{u}}, \bar{\mathbf{u}}\}$ lower and upper actuator command limits (length changes). In [9] the derivation of the actuation sensitivity matrices is formulated through the Integrated Force

Method. Alternatively, using the Direct Stiffness Method:

$$\begin{aligned}\mathbf{S}^{q} &= \mathbf{C}\ \mathbf{K}^{-1}\mathbf{B}^{eq}\mathbf{K}^{act} = \mathbf{B}^{u} \\ \mathbf{S}^{N} &= \mathbf{K}^{el}\mathbf{B}^{eqT}\mathbf{C}\ \mathbf{K}^{-1}\mathbf{B}^{eq}\mathbf{K}^{act} = \mathbf{K}^{el}\mathbf{B}^{eqT}\mathbf{B}^{u}\end{aligned} \tag{34}$$

The solution of the constrained minimization problem stated in (33) is the input commands $\mathbf{u}$ for a given set of actuators S^{act}. The efficacy of a candidate actuator eff_{ij}^{u} is quantified by evaluating the effect of each actuator command in turn u_{ji} for the load case j. Depending on the control objective, the efficacy is the ratio between the displacement (Δq) or force (ΔN) change caused by u_{ji} and the desired output correction $\mathbf{\Delta y}_{j}^{SLS}$:

$$eff_{ij}^{u} = \frac{\sum_{k=1}^{n^{y}} \left(\mathbf{S}_{ki}^{\#}\ u_{ji}\right) \odot \frac{1}{\mathbf{\Delta y}_{j}^{SLS}}}{n^{y}}; \quad \begin{array}{l} \#q \text{ or } N \\ k = \text{output index} \\ i = \text{actuator index} \\ j = \text{load case} \end{array} \tag{35}$$

where $\odot$ denotes the Hadamard product (i.e., elementwise). The actuator efficacy is then averaged for all load cases:

$$Eff_{i} = \frac{\sum_{j=1}^{LC} eff_{ji}^{u}}{n^{LC}} \tag{36}$$

In [13] the number of actuators n^{act} is predetermined, then the n^{act} element with the highest efficacy are selected to house the actuators. In this work, similarly to the process described in Section 3.1, a greedy algorithm is employed to solve the actuator placement problem stated in (24) where $(1 - Eff\left(S^{act}\right))$ is taken as the objective function. $Eff\left(S^{act}\right)$ is the global efficacy computed for an entire set of actuators. Starting from a set containing all elements, the actuator that has the lowest efficacy is discarded iteratively. Alternatively, starting from an empty set, the actuator that has the highest efficacy is added iteratively. When the efficacy is evaluated for each element in turn, it will be referred to single element efficacy S.A.E, while with M.A.E. the efficacy is evaluated for multiple actuators $Eff\left(S^{act}\right)$. Using S.A.E., the control inputs are computed n^{el}-1 times. When using M.A.E., the actuator commands must be recomputed for all permutations, which requires a significant computational cost for structures made of many elements. The solution layout with the smallest number of actuators that satisfy the target output as well as force and energy constraints, as stated in (24), is selected. The formulation given in [13] is referred to as direct single-element efficacy D.S.A.E since the number of actuators is predetermined. The minimization problem expressed in (33) can be separated in displacement and force control for better comparison with the method presented in Section 3.1.

Constrained displacement control

The minimization problem for displacement compensation is given by:

$$\min_{\mathbf{u}} \left\| \mathbf{K}^{-1}\mathbf{B}^{u}\mathbf{u} - \mathbf{\Delta y}^{SLS} \right\|_{2};\ \underline{\mathbf{u}} \le \mathbf{u} \le \overline{\mathbf{u}} \tag{37}$$

Constrained force control

As described in [9], the optimal compatible internal force distribution is given by the following minimization problem:

$$\min_{\mathbf{N}} \left\| \mathbf{B}^{eq}\mathbf{N} - \mathbf{z} \right\|_2 \; s.t. \; \mathbf{A}\underline{\sigma} \le \mathbf{N} \le \bar{\sigma}\mathbf{A} \tag{38}$$

where $\{\underline{\sigma}, \bar{\sigma}\}$ are the stress limits. The optimal control inputs are given by the following minimization problem:

$$\min_{\mathbf{u}} \left\| (\mathbf{K}^{el}\mathbf{B}^{eqT}\mathbf{K}^{-1}\mathbf{B}^{u} + \mathbf{D})\mathbf{u} - \Delta\mathbf{N} \right\|_2 ; \; \underline{\mathbf{u}} \le \mathbf{u} \le \bar{\mathbf{u}} \tag{39}$$

where $\Delta\mathbf{N} = \mathbf{N} - \mathbf{N}^0$ is the required force redirection from the uncontrolled state $\mathbf{N}^0$.

4 CASE STUDY

The two actuator placement methods given in Section 3 are benchmarked using a prismatic truss structure that is 36 m in height and has a slenderness ratio of 12, Figure 2 illustrates displacement and internal force control for different actuator layouts. The actuator length changes modify the displacement response to reduce excessive deformations under lateral loading within the prescribed serviceability limit.

Assuming each floor is modeled with a rigid diaphragm, floor elements are omitted by applying internal horizontal constraints on the corresponding degrees of freedom. This way the free DOFs are reduced from 72 to 42. The structural elements have a cylindrical hollow section. There is a total of 72 elements. Four wind-like lateral load cases are considered applied on each side of the building. Following [13], the structural elements are sized to satisfy ultimate limit states (ULS), while serviceability limit states (SLS) do not have any influence on element sizing because they are satisfied through active control. The displacement limits are set to H_f /500 where H_f is the height of each floor f.

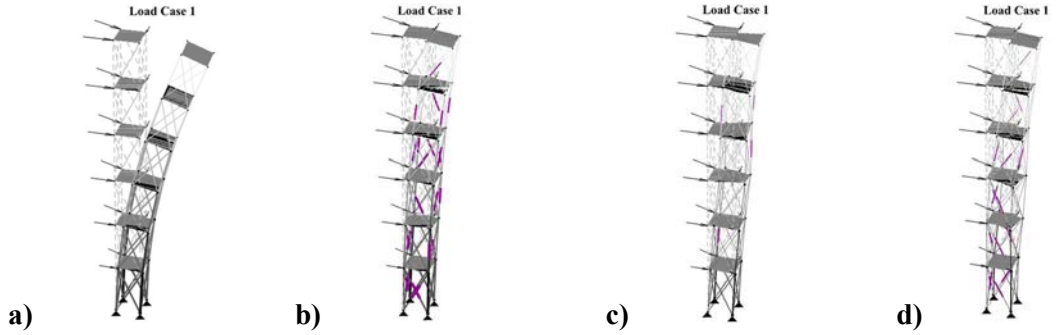

Figure 2 a) Uncontrolled displacements, **b)** Controlled displacements (opt. layout through M.A.E.), **c)** Controlled displacements through active columns, **d)** Controlled displacements through active diagonals.

Figure 2 illustrates displacement and internal force control for different actuator layouts. The actuator length changes modify the displacement response to reduce excessive deformations under lateral loading within the prescribed serviceability limit.

Four performance metrics are considered: 1) the trace $\mathrm{tr}(\widetilde{\mathbf{W}}_j)$ and 2) maximum eigenvalue

$\lambda_{max}(\widetilde{\mathbf{W}}_j)$ of the compensability Gramian, which are related to the mean and maximum squared error of the controlled system, 3) the maximum actuator force F_{max} and the 4) average control energy E_{mean}. Figure 3 shows the variation of each metric with the number of actuators for displacement and force control respectively. The upper ↑ and lower ↓ indicate the ascending or descending greedy optimization process employed to obtain the actuator layout. Table 1 collects performance metrics for the actuator layouts produced by each method. To benchmark solutions produced using different metrics, a solution with the same number of actuators and that satisfies the target output (i.e., displacements) is selected, while actuator force and energy constraints are released.

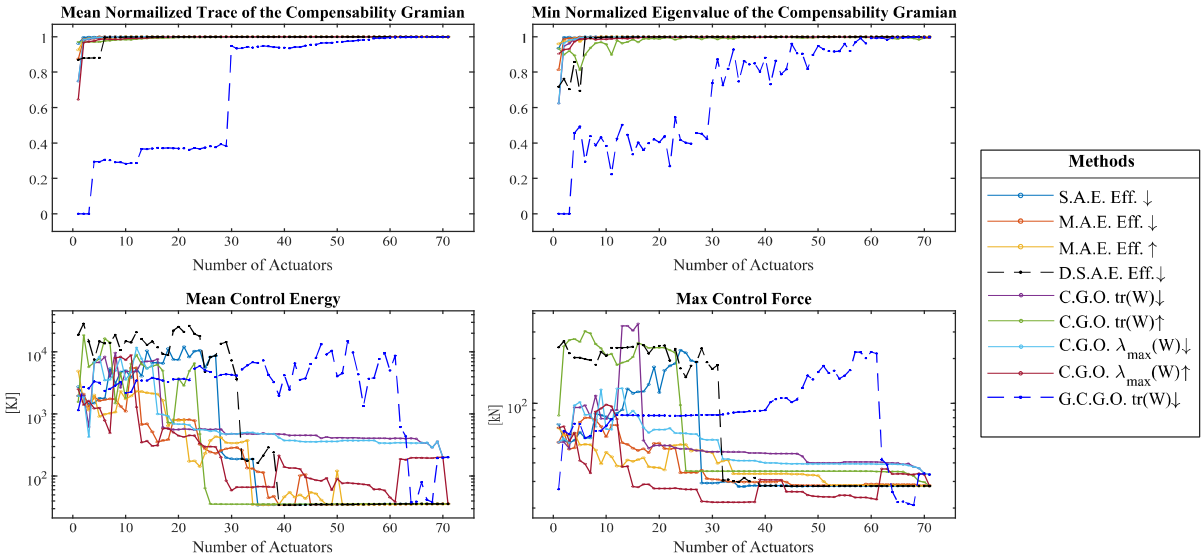

Figure 3 Actuation placement metrics for displacement control

Table 1: Solution layout metrics for displacement control

Method	Selection Metric	Direction	n^{act}	F_{max} [kN]	E_{mean} [KJ]	tr(W)	λ_{max}(W)	Active Diagonals
S.A.E.	Eff.	↓	22	176.2	8287.5	1.000	1.000	15
M.A.E.	Eff.	↓	22	44.1	809.9	1.000	1.000	18
M.A.E.	Eff.	↑	22	43.0	174.1	1.000	1.000	19
D.S.A.E.	Eff.	-	22	41.0	3511.1	1.000	1.000	17
C.G.O.	tr(W)	↓	22	43.6	568.0	1.000	1.000	9
C.G.O.	tr(W)	↑	22	227.2	4928.4	0.996	0.993	6
C.G.O.	λ_{max}(W)	↓	22	39.3	667.1	1.000	1.000	9
C.G.O.	λ_{max}(W)	↑	22	21.1	453.8	0.999	0.998	16
D.I.C.G.O. *	tr(W)	↓	22	179.6	26319.4	0.361	0.280	10
Force constrained actuator placement (F^{act} < 50 kN)								
M.A.E.	Eff.	↑	12	47.6	340	1.000	1.000	8
C.G.O.	tr(W)	↓	11	49.1	1304	1.000	1.000	0

Actuator layouts produced by methods that consider specific load cases have significantly higher performance compared to methods that are independent of the disturbance. This is

somewhat expected because the placement is determined to perform best for a smaller subset of cases. All metrics related to the compensability Gramian do not differ significantly when a high number of active elements is considered. A similar issue occurs, albeit to a lesser extent, when the selection is based on the global efficacy measure Eq (36) evaluated for the entire actuator set. Generally, the efficacy measures provide a well-weighted assessment of the control error. Compensability Gramian-related metrics tend to overestimate the response states that require larger compensation while underestimating response states that require small compensation. When the efficacy is evaluated for a single actuator, ranking and subsequent selection require minimum computational cost since the optimal inputs are computed only at the start of each step (S.A.E.), or only once (D.S.A.E.) instead of multiple permutations. The choice of the greedy process direction (ascending or descending) depends on the maximum number of actuators since choices made at an early stage are often counterproductive later. For example, for placement with a low number of actuators, it is more convenient to start from an empty set and vice versa. Solutions that do not satisfy the target output are indicated with *. For the case study considered here, 4 active columns are sufficient to satisfy the displacement limits. A larger number of active diagonals (16) is required to achieve a similar control output error albeit using significantly lower energy (870 kJ instead of 1794 kJ) and actuator forces (42 kN instead of 61 kN). Descending greedy algorithms favor active diagonal locations initially, but their performance becomes unstable as the number of actuators is reduced. Typically, it is not possible to assign columns as active elements if they are eliminated at early search stages. Differently, ascending algorithms can “make up” for early choices later in the process by adding active diagonals that were initially not selected. If the maximum actuator force is limited to 50 kN, the two methods that provide the layouts with the lowest number of actuators satisfying all limit states, are the ascending M.A.E. and the descending C.G.O. and the former requires the least control energy.

5 CONCLUSIONS

Actuator placement techniques typically use optimization algorithms to determine the optimal layout. Depending on the control objective and requirements, different metrics and constraints can be considered. Actuator layouts produced by considering only displacement or force compensability separately are often not practical due to power and actuation force constraints. Since the design of a civil structure is typically carried out under the assumption of well-defined load cases, the design of the control system should be no different. This work has shown that actuator placement considering specific load cases, generally, produces better-quality solutions in terms of control efficacy and feasibility. Control efficacy evaluated for a single actuator provides a clear measure of the actuator's contribution to the control target. Differently, with compensability Gramian-related metrics, and especially when using many actuators, the difference in optimization metrics between two similar actuator layouts is practically negligible. This issue could be solved by adding further constraints for the determination of the actuator commands. Future work will implement an extension of the Gramian-based formulation to include actuation force limits as well as considering energy minimization. Generally, constrained optimization of the control inputs allows for a better

evaluation of performance metrics within similar sets. To overcome the limitations of the optimization process based on greedy algorithms implemented in this paper, future work will investigate global search methods including stochastic and mixed-integer programming.

6 ACKNOWLEDGMENTS

This work has been funded by the German Research Foundation (DFG-Deutsche Forschungsgemeinschaft) as part of the Collaborative Research Center 1244 (SFB 1244) *Adaptive Skins and Structures for the Built Environment of Tomorrow*.

REFERENCES

[1] United Nations Environment Programme, "Sand, Rarer than One Thinks: UNEP Global Environmental Alert Service (GEAS) - March 2014," 2014, [Online]. Available: https://wedocs.unep.org/20.500.11822/8665

[2] IEA and UNEP, "2019 Global Status Report for Buildings and Construction," 2019.

[3] A. Preumont and Kazuto Seto, *Active Control of Structures*. Wiley, 2008.

[4] A. P. Reksowardojo, G. Senatore, A. Srivastava, C. Carroll, and I. F. C. Smith, "Design and testing of a low-energy and -carbon prototype structure that adapts to loading through shape morphing," *Int. J. Solids Struct.*, p. 111629, May 2022, doi: 10.1016/j.ijsolstr.2022.111629.

[5] L. Blandini *et al.*, "D1244: Design and Construction of the First Adaptive High-Rise Experimental Building," *Front. Built Environ.*, vol. 8, 2022, Accessed: Jul. 01, 2022. [Online]. Available: https://www.frontiersin.org/article/10.3389/fbuil.2022.814911

[6] G. Cazzulani, F. Ripamonti, and F. Resta, "Fatigue damage reduction for flexible structure through active control," in *2014 IEEE Conference on Control Applications (CCA)*, Juan Les Antibes, France: IEEE, Oct. 2014, pp. 1729–1734. doi: 10.1109/CCA.2014.6981562.

[7] S. Steffen, A. Zeller, M. Böhm, O. Sawodny, L. Blandini, and W. Sobek, "Actuation concepts for adaptive high-rise structures subjected to static wind loading," *Eng. Struct.*, vol. 267, p. 114670, Sep. 2022, doi: 10.1016/j.engstruct.2022.114670.

[8] S. Steffen, L. Blandini, and W. Sobek, "Analysis of the inherent adaptability of basic truss and frame modules by means of an extended method of influence matrices," *Eng. Struct.*, vol. 266, p. 114588, Sep. 2022, doi: 10.1016/j.engstruct.2022.114588.

[9] G. Senatore and A. P. Reksowardojo, "Force and Shape Control Strategies for Minimum Energy Adaptive Structures," *Front. Built Environ.*, vol. 6, p. 105, Jul. 2020, doi: 10.3389/fbuil.2020.00105.

[10] J. L. Wagner *et al.*, "On steady-state disturbance compensability for actuator placement in adaptive structures," - *Autom.*, vol. 66, no. 8, pp. 591–603, Aug. 2018, doi: 10.1515/auto-2017-0099.

[11] M. Bohm *et al.*, "Input modeling for active structural elements - extending the established FE-Work?ow for modeling of adaptive structures," in *2020 IEEE/ASME International Conference on Advanced Intelligent Mechatronics (AIM)*, Boston, MA, USA: IEEE, Jul. 2020, pp. 1595–1600. doi: 10.1109/AIM43001.2020.9158996.

[12] Y. Wang and G. Senatore, "Design of adaptive structures through energy minimization: extension to tensegrity," *Struct. Multidiscip. Optim.*, vol. 64, no. 3, Art. no. 3, Sep. 2021, doi: 10.1007/s00158-021-02899.

[13] G. Senatore, P. Duffour, and P. Winslow, "Synthesis of minimum energy adaptive structures," *Struct. Multidiscip. Optim.*, vol. 60, no. 3, Art. no. 3, Sep. 2019, doi: 10.1007/s00158-019-02224-8.

[14] F. Pasqualetti, S. Zampieri, and F. Bullo, "Controllability metrics, limitations and algorithms for complex networks," in *2014 American Control Conference*, Portland, OR, USA: IEEE, Jun. 2014, pp. 3287–3292. doi: 10.1109/ACC.2014.6858621.

[15] Y. Wang and G. Senatore, "Minimum energy adaptive structures – All-In-One problem formulation," *Comput. Struct.*, vol. 236, p. 106266, Aug. 2020, doi: 10.1016/j.compstruc.2020.106266.